arXiv:cond-mat/0507338v1 [cond-mat.str-el] 14 Jul 2005

Field-Dependent Hall Effect in Single Crystal Heavy Fermion YbAgGe below 1K

S.L. Bud'ko*, V.Zapf†, E. Morosan*, and P.C. Canfield*

*Ames Laboratory US DOE and Department of Physics and Astronomy, Iowa State University, Ames, IA 50011, USA

†MS E536, National High Magnetic Field Laboratory - Los Alamos National Laboratory, Los Alamos, NM 87545, USA

(Dated: February 2, 2008)

Abstract

We report the results of a low temperature ($T \geq 50$ mK) and high field ($H \leq 180$ kOe) study of the Hall resistivity in single crystals of YbAgGe, a heavy fermion compound that demonstrates field-induced non-Fermi-liquid behavior near its field-induced quantum critical point. Distinct features in the anisotropic, field-dependent Hall resistivity sharpen on cooling down and at the base temperature are close to the respective critical fields for the field-induced quantum critical point. The field range of the non-Fermi-liquid region decreases on cooling but remains finite at the base temperature with no indication of its conversion to a point for $T \rightarrow 0$. At the base temperature, the functional form of the field-dependent Hall coefficient is field direction dependent and complex beyond existing simple models thus reflecting the multi-component Fermi surface of the material and its non-trivial modification at the quantum critical point.

PACS numbers: 72.15.Qm, 72.15.Gd, 75.30.Mb, 75.20.Hr

I. INTRODUCTION

YbAgGe was recently recognized to be one the few stoichiometric Yb-based heavy fermion compounds that demonstrate field-induced non-Fermi-liquid (NFL) behavior as evidenced by thermodynamic and transport measurements in an applied magnetic field [1]. In zero applied field YbAgGe has two (small magnetic moment) magnetic ordering transitions, at ≈ 1 K and ≈ 0.65 K (first order) [1, 2, 3]. The magnetic ordering temperatures are well separated from the Kondo temperature ($T_K \sim 25$ K) that is well below estimated CEF splitting ($T_{CEF} \sim 60 - 100$ K) [4, 5]. The critical field needed to reach the quantum critical point (QCP) in YbAgGe is moderate and anisotropic ($H_c^{ab} \approx 45$ kOe, $H_c^c \approx 80$ kOe) [1, 3]. Hall effect measurements through the QCP have been suggested [6] to be one of the key experiments to distinguish between two general descriptions of an antiferromagnetic QCP: (1) spin-density-wave and (2) composite heavy fermion (HF) scenarios. Initial (down to 0.4 K) Hall effect measurements on YbAgGe [7] show clear local maxima/minima (for $H\|ab/H\|c$, respectively) in the field-dependent Hall resistivity, $\rho_H(H)$, that occur at values that approach the respective critical fields as $T \to 0$. The feature in $\rho_H(H)$ establishes a new, distinct, line in the anisotropic $H - T$ phase diagrams of YbAgGe [7]. A similar, additional, Hall-effect line was detected in $YbRh_2Si_2$ [8], the other Yb-based compound that is perceived to be a well established example of a material with a field-induced QCP [9]. For $YbRh_2Si_2$, the gradual change of the Hall coefficient, R_H, in an applied field was interpreted [8] as extrapolating to a sudden jump at the QCP in the zero temperature limit and hence suggesting that the composite HF scenario [6] is realized in this material. As distinct from $YbRh_2Si_2$, the field-dependent Hall coefficient in YbAgGe, even above 0.4 K (the base temperature in our previous study), had a rather complex, albeit fairly sharp, feature at H_c, clearly different for the field-induced QCP for $H\|ab$ and $H\|c$ [7]. Extension of the temperature range of the Hall effect measurements down to 50 mK in temperature allows us to observe the evolution of the field-dependent Hall coefficient much closer to the $T = 0$ QCP. In this work we expanded the probed $H-T$ space down to $T/T_N \sim 0.05$ and up to $H/H_{QCP} \sim 2-4$ that exceeds considerably our previous capabilities as well as, in relative $(T/T_N, H/H_{QCP})$ terms, the phase space accessed in Hall measurements on $YbRh_2Si_2$ [8].

II. EXPERIMENTAL

YbAgGe single crystals in the form of clean, hexagonal-cross-section rods of several mm length and up to 1 mm^2 cross section were grown from high temperature ternary solutions rich in Ag and Ge (see [2] for details of the samples' growth). Their structure and full site-occupancy without detectable site-disorder were confirmed by single crystal X-ray diffraction [10]. The four-probe Hall resistivity measurements $\rho_H(H)|_T$ were performed on two pairs of the samples: (i)$H\|[120]$, $I\|[001]$ with the Hall voltage, V_H, measured along [100]; (ii)$H\|[001]$, $I\|[100]$ with V_H measured along [120]. One sample in each pair was exactly the same sample as studied in Ref. 7. The measurements were performed at temperatures down to 50 mK and magnetic fields up to 180 kOe using a ^{3}He-^{4}He dilution refrigerator in a 200 kOe Oxford Instruments superconducting magnet system at the National High Magnetic Field Laboratory in Los Alamos. The samples were immersed in the ^{3}He-^{3}He mixture together with a field-calibrated RuO_2 thermometer, thus providing excellent thermalization and allowing for use of higher excitation currents to achieve better signal to noise ratio. The Hall resistance was measured with a Linear Research LR-700 ac resistance bridge with excitation currents of 1-3 mA (no additional sample heating was detected at the base temperature and above at these current values). For most of the runs the protocol of the measurements was the following: the temperature was stabilized at the desired value with the 180 kOe (-180 kOe) field applied, then the measurements were taken while the field was swept at 2 kOe/min rate through zero to -180 kOe (180 kOe). Magnetic flux jumps in the 200 kOe superconducting magnet drastically increase the noise in the data taken in applied field below $\sim$ 20 kOe, so only data for $H \geq 20$ kOe will be presented. To eliminate the effect of inevitable (small) misalignment of the voltage contacts, the Hall measurements were taken for two opposite directions of the applied field, H and $-H$, and the odd component, $(\rho_H(H) - \rho_H(-H))/2$ was taken as the Hall resistivity, $\rho_H(H)$. Since, within the error bars of the measured geometry of the samples and contact positions, both samples in each pair yielded the same results, for ease of comparison in the following we will present the data for the samples used in Ref. 7.

The protocol of the measurements adopted in this work, whereas time-conserving, resulted in an artifact (originating from the hysteretic component of the magnetoresistance at the lower magnetic transition [1, 2, 3], which is not eliminated completely through the Hall

resistivity calculations described above in the measurements protocol used for the most of the measurements) seen in the low temperature $\rho_H(H)$ data for $H\|c$ at approximately 20-30 kOe (see Fig. 1(b) below). Whereas we kept this artifact in $\rho_H(H)$ data 1(b) for illustrative purpose, subsequent data for $H\|c$ were truncated to $\sim$ 30 kOe. For $H\|ab$ a similar feature occurs below $\sim$ 20 kOe, in the region of magnetic flux jumps noise.

III. RESULTS AND DISCUSSION

Field-dependent Hall resistivities for $H\|ab$ and $H\|c$ at temperatures between 50 and 750 mK are shown in Fig. 1. In the overlapping temperature region, the current data are consistent with that reported in Ref. 7. On cooling down, the main feature in the $\rho_H(H)$ sharpens for both orientations of the applied field. For $H\|ab$, in addition to sharpening, a plateau in $\rho_H(H)$ emerges from the data for $T < 400$ mK in the approximate range of fields 60 kOe $< H <$ 90 kOe.

Representative field-dependent Hall coefficients (calculated as $d\rho_H/dH$ from the sub-set of the data in Fig. 1) are shown in Fig. 2. As in the case of Hall resistivities, the features associated with the proximity to field induced QCP are sharper and better-defined at lower temperatures. In comparison to the initial study [7], lower temperatures, higher fields and better signal-to-noise ratio of the current data allow us to consider more than one feature in the Hall resistivity and Hall coefficient (Fig. 3). The least ambiguous feature is a sharp maximum/minimum ($H\|ab/H\|c$) in the anisotropic Hall resistivity (a). The two extrema in $d\rho_H/dH$, (b) and (c), are associated with the main feature in ρ_H and are, in a broad sense, a measure of the width of the respective feature. Clear breaks of the slope ((d), (e) for $H\|ab$, (e) for $H\|c$) are seen at higher fields. It is noteworthy that for $H^{ab} > H_e$ and $H^c > H_e$ the Hall coefficient, $R_H = d\rho_H/dH$, is practically field-independent, suggesting these fields to be a caliper of the material entering into Fermi-liquid state and as such approximately defining the coherence line on the $H - T$ phase diagram (alternatively plotted for this material in Refs. 1, 7 as the temperature up to which the resistivity obeys $\rho(T) = \rho_0 + AT^2$ law). Finally, for $H\|c$ there is a relatively broad (even at the base temperature) maximum (f) in the Hall resistivity, however, since there is no corresponding feature in $d\rho_H/dH$ (lower panel of Fig. 3(b)) it is not so likely that this maximum corresponds to a phase boundary or crossover.

Based on the measurements and salient features discussed above, considered together with the thermodynamic and transport data in an applied field at temperatures down to 400 mK [1], the magnetotransport measurements down to 70 mK [11] and our earlier Hall measurements down to 400 mK [7], we can construct anisotropic low-temperature $H-T$ phase diagrams for YbAgGe (Fig. 4). For a discussion related to the complexity of the magnetically ordered phases, we refer the reader to the original works [1, 2, 3, 7, 11]. The Hall line defined from the maximum/minimum ($H\|ab/H\|c$) of the Hall resistivity at low temperatures approaches the QCP. The width of the Hall anomaly related to the QCP (defined here as the region between two relevant extrema, (b) and (c) in Fig. 3, in $d\rho_H/dH$) decreases on cooling down and reaches $\approx 0.2H_{crit}$ at the base temperature, being much narrower, in relative units, than for $YbRh_2Si_2$ [8]. For both orientations of the applied field the Hall anomaly in YbAgGe can be followed up to $2-3$ K, far beyond the ordering temperature in zero field. At low temperatures, the lower-field boundary of the Hall anomaly initially follows the magnetic phase boundary (Fig. 4) and then departs from this boundary and continues singly to higher temperatures.

Hall measurements in an extended $H-T$ range suggest an existence of additional boundaries on the phase diagrams. For $H\|ab$ (Fig. 4(a)), almost temperature-independent lines at $\sim$ 70 kOe and $\sim$ 120 kOe are suggested by following two high-field kinks in $d\rho_H/dH$. Above $\sim$ 1 K there features are smeared out and are difficult to follow further. The Hall coefficient becomes field-independent above the 120 kOe line. The line starting at $\sim$ 120 kOe can be easily extended to accommodate the coherence temperature points defined from the magnetotransport $\rho(T)|_H$ data in Ref. 1 into a common phase boundary. For $H\|c$ (Fig. 4(b)) $d\rho_H/dH \approx const$ for fields above the line that corresponding to $\sim$ 150 kOe at the base temperature. Similarly to the case of $H\|ab$ above, this line can be used to re-define the coherence line for $H\|c$ and shift it to higher fields compared to its tentative position inferred from the limited $\rho(T)|_H$ data [1] taken in significantly smaller $H-T$ domain. It is worth noting that Figures 4(a) and 4(b) indicate that there appears to be a finite range of fields, even as $T \to 0$, over which NFL appears. This is rather remarcable and needsw further theoretical, as well as experimental, study.

Whereas the general features of the phase diagram discussed so far and their evolution with temperature are, at a gross level, similar for both orientations of the applied field, the functional form of the field-dependent Hall coefficient (Fig. 2), differs between $H\|ab$

and $H\|c$, and is disparate to the theoretically suggested options [6] and the observations in $YbRh_2Si_2$ [8]. Whereas the level of similarity between the field-induced NFL behavior in YbAgGe and $YbRh_2Si_2$ is open for debate, it is of note that the Hall resistivity (or Hall coefficient) in real materials has a complex dependence on the details of the electronic structure (see *e.g.* Refs. 12, 13). Even in a simpler (but somewhat related) case of the electronic topological transition (ETT) [14, 15], in the absence of strong electronic correlations, an accurate prediction (based on band-structure calculations) of the change of the Hall coefficient as a function of the parameter controlling the ETT may be an intricate task [16]. With this in mind, the differences in functional behavior of the Hall coefficient for two orientations of the applied field in YbAgGe is probably due to the details of the complex anisotropic Fermi surface of this material, while the distinct feature for each direction of the applied field is associated with the field-induced QCP in this material.

IV. SUMMARY

Distinct features in the Hall resistivity of YbAgGe for two orientations of the applied magnetic field, $H\|ab$ and $H\|c$, were followed down to $T = 50$ mK. The features sharpen on cooling down and at the base temperature are close to the respective critical fields for the field induced QCP. New lines are being suggested for the composite $H - T$ phase diagrams. The non-Fermi-liquid part of the $H - T$ phase diagram apparently remains finite in the limit of $T \to 0$ suggesting that the topology of the phase diagram in the vicinity of the field-induced QCP in YbAgGe is different from most commonly acknowledged cases.

Acknowledgments

Ames Laboratory is operated for the U.S. Department of Energy by Iowa State University under Contract No. W-7405-Eng.-82. This work was supported by the Director for Energy Research, Office of Basic Energy Sciences. Work at the NHMFL - Los Alamos was performed under the auspices of the NSF, the state of Florida and the U.S. Department of Energy.

---

[1] S. L. Bud'ko, E. Morosan, and P. C. Canfield, Phys. Rev. B **69**, 014415 (2004).

[2] E. Morosan, S. L. Bud'ko, P. C. Canfield, M. S. Torikachvili, and A. H. Lacerda, J. Magn. Magn. Mat. **277**, 298 (2004).

[3] K. Umeo, K. Yamane, Y. Muro, K. Katoh, Y. Niide, A. Ochiai, T. Morie, T. Sakakibara, and T. Takabatake, J. Phys. Soc. Jpn. **73**, 537 (2004).

[4] K. Katoh, Y. Mano, K. Nakano, G. Terui, Y. Niide, and A. Ochiai, J. Magn. Magn. Mat. **268**, 212 (2004).

[5] T. Matsumura, H. Ishida, T. J. Sato, K. Katoh, Y. Niide, and A. Ochiai, J. Phys. Soc. Jpn. **73**, 2967 (2004).

[6] P. Coleman, C. Pépin, Q. Si, and R. Ramazashvili, J. Phys.: Cond. Mat. **13**, R723 (2001).

[7] S. L. Bud'ko, E. Morosan, and P. C. Canfield, Phys. Rev. B **71**, 054408 (2005).

[8] S. Paschen, T. Lühmann, S. Wirth, P. Gegenwart, O. Trovarelli, C. Geibel, F. Steglich, P. Coleman, and Q. Si, Nature **432**, 881 (2004); *ibid.* **431**, 1022 (2004).

[9] P. Gegenwart, J. Custers, T. Tayama, K. Tenya, C. Geibel, G. Sparn, N. Harrison, P. Kerschl, D. Eckert, K.-H. Müller, et al., J. Low Temp. Phys. **133**, 3 (2003).

[10] Y. Mozharivskyj, private communication.

[11] P. G. Niklowitz, G. Knebel, J. Flouquet, S. L. Bud'ko, and P. C. Canfield, cond-mat/0507211.

[12] D. V. Livanov, Phys. Rev. B **60**, 13439 (1999).

[13] F. D. M. Haldane (2005), arXiv:cond-mat/0504227.

[14] A. A. Varlamov, V. S. Egorov, and A. V. Pantsulaya, Adv. Phys. **38**, 469 (1989).

[15] Y. M. Blanter, M. I. Kaganov, A. V. Pantsulaya, and A. A. Varlamov, Phys. Reports **245**, 159 (1994).

[16] D. V. Livanov, E. I. Isaev, Y. K. Vekilov, S. I. Manokhin, A. S. Mikhaylushkin, and S. I. Simak, Eur. Phys. J. B **27**, 119 (2002).

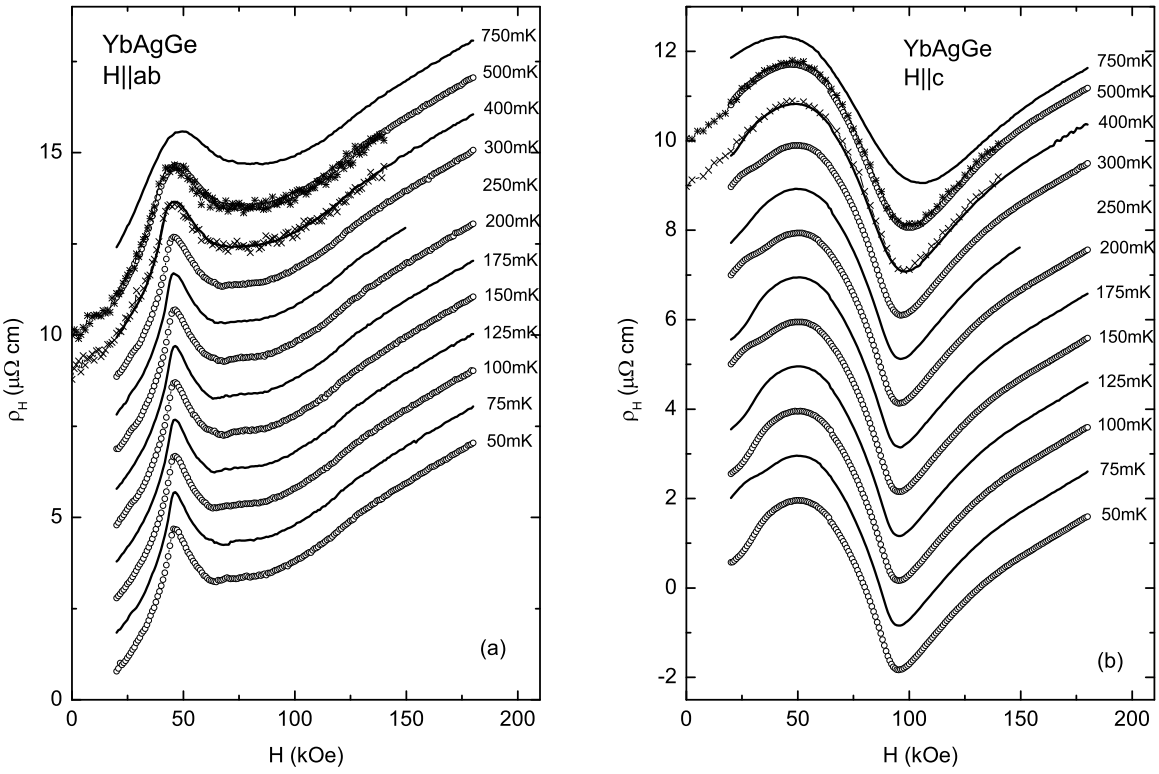

FIG. 1: Field-dependent Hall resistivity of YbAgGe ((a) - $H\|ab$, (b) - $H\|c$) measured at different temperatures. The curves, except for $T = 50$ mK, are shifted by $1\mu\Omega$ cm increments for clarity. For 400 mK and 500 mK, data from our initial measurements [7] are shown by $\times$ and $*$ for comparison. Note: for (b) the feature located near $H = 20 - 30$ kOe is an artifact of the measurements protocol and hysteresis in magnetoresistivity at the lower transition (see text).

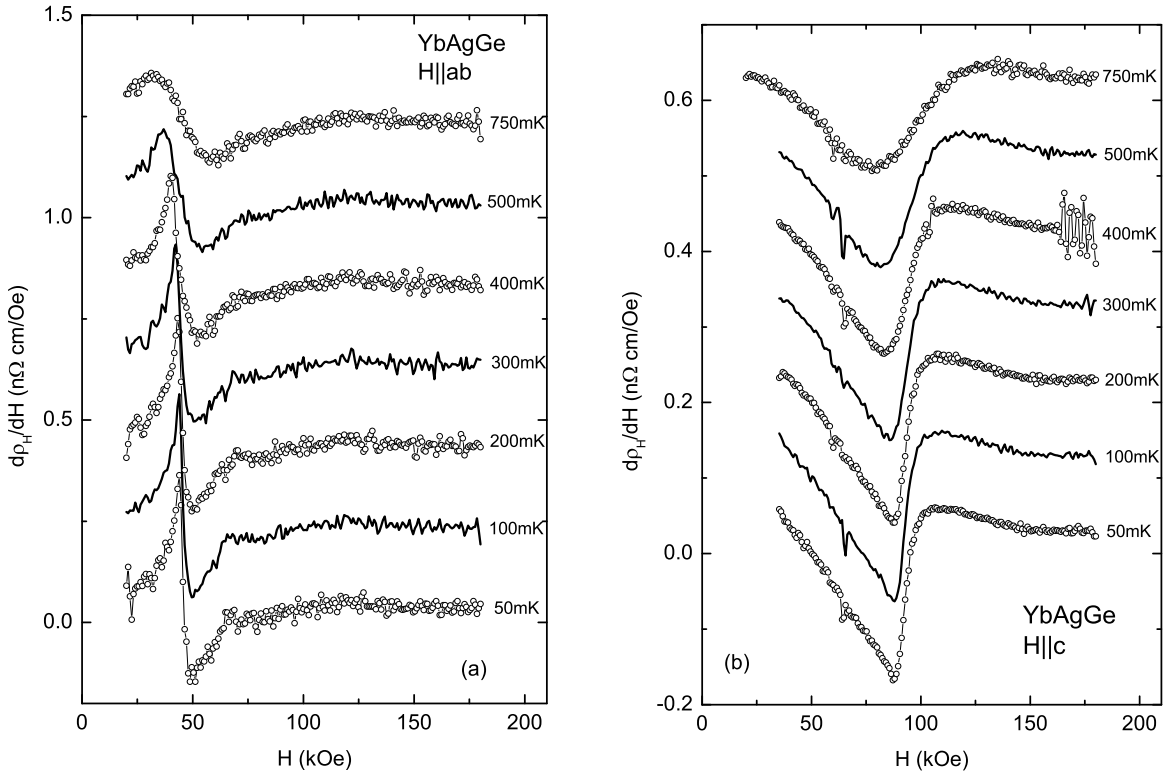

FIG. 2: Field-dependent Hall coefficient of YbAgGe ((a) - $H\|ab$, (b) - $H\|c$), defined as $R_H = d\rho_H/dH$, measured at different temperatures. The curves, except for $T = 50$ mK, are shifted by (a) 0.2 nΩ cm/Oe and (b) 0.1 nΩ cm/Oe increments for clarity. Low field data in (b) (except for 750 mK, above the lover magnetic transition) are truncated below ~ 30 kOe (see text).

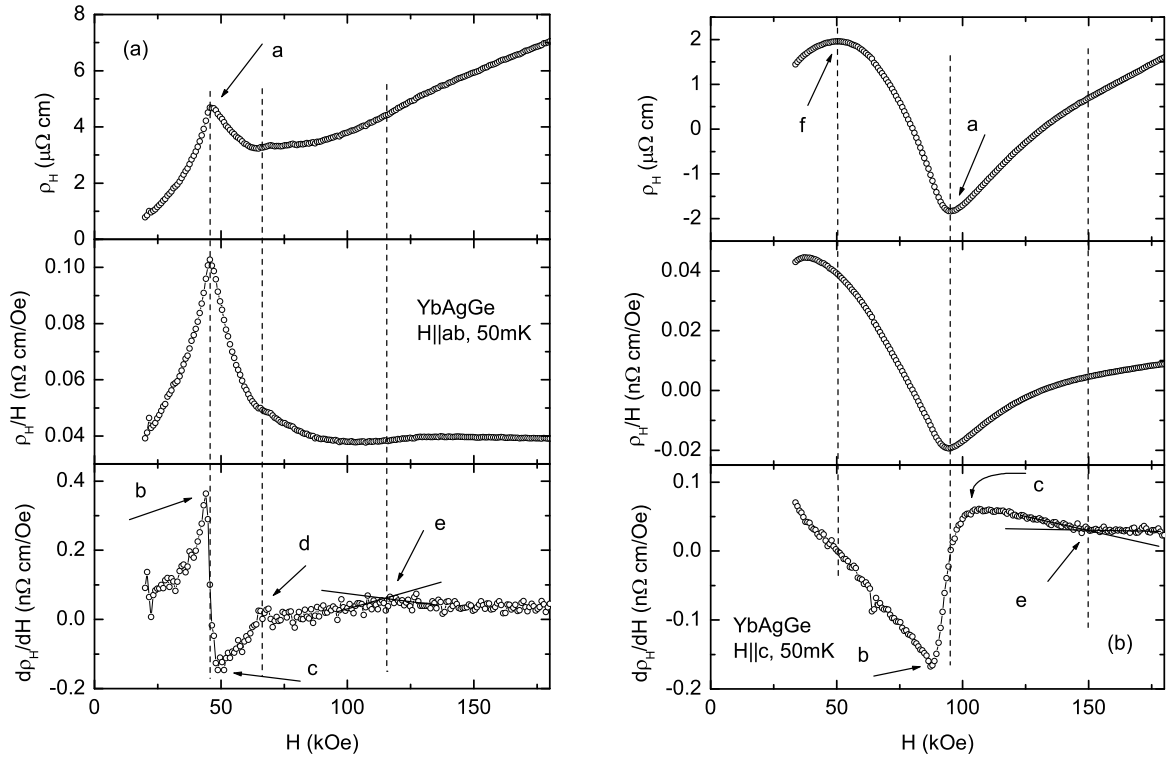

FIG. 3: Field-dependent Hall resistivity (ρ_H), Hall resistivity divided by field (ρ_H/H) and Hall coefficient ($d\rho_H/dH$) of YbAgGe ((a) - $H\|ab$, (b) - $H\|c$) at $T = 50$ mK. Arrows and letters mark different features of the curves (see text for the discussion).

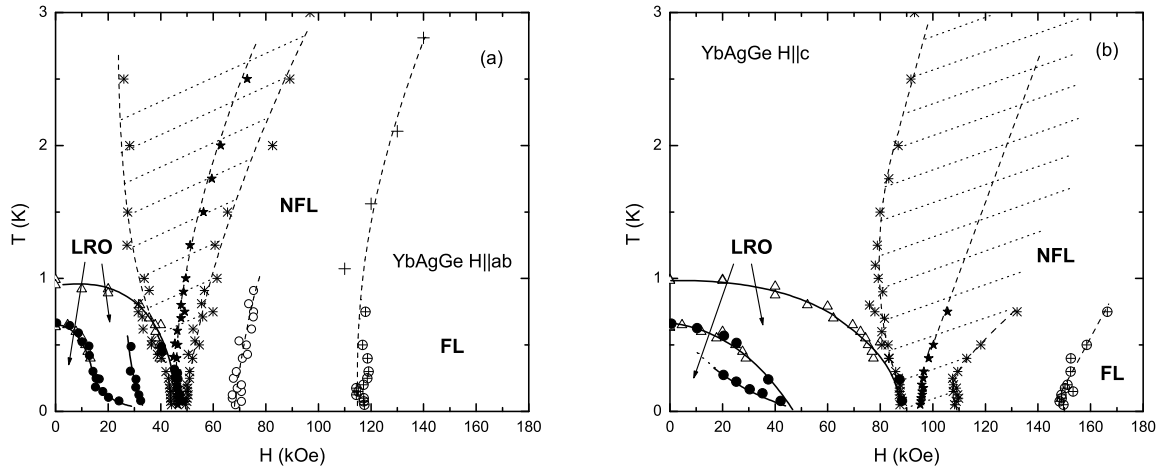

FIG. 4: Composite anisotropic $H-T$ phase diagrams for YbAgGe: (a) $H\|ab$, (b) $H\|c$. Symbols: $\triangle$ - magnetic transitions from thermodynamic and magneto-transport measurements in Ref. 1; $\bullet$ - magnetic transitions from magneto-transport measurements in Ref. 11; solid lines - tentative magnetic phase boundaries; + - coherence line defined as a high temperature limit of the region of $\rho(T) = \rho_0 + AT^2$ resistivity behavior [1]; $\bigstar$ - Hall line defined from the maximum/minimum ($H\|ab/H\|c$) of the Hall resistivity ((a) in Fig. 3); $*$ - lines defined from the maximum and minimum in $d\rho_H/dH$ ((b) and (c) in Fig. 3), area between these lines is accentuated by hatching; $\circ, \oplus$ in panel (a) and $\oplus$ in panel (b) - point corresponding to high field break of the slope in $d\rho_H/dH$ ((d) and (e) in Fig. 3(a) and (d) in Fig. 3(b)). Dashed lines are guide for the eye.